

N O T I C E

THIS DOCUMENT HAS BEEN REPRODUCED FROM
MICROFICHE. ALTHOUGH IT IS RECOGNIZED THAT
CERTAIN PORTIONS ARE ILLEGIBLE, IT IS BEING RELEASED
IN THE INTEREST OF MAKING AVAILABLE AS MUCH
INFORMATION AS POSSIBLE



Technical Memorandum **80568**

(NASA-TM-80568) COMPARISON OF MAGNETIC
ANOMALIES OF LITHOSPHERIC ORIGIN MEASURED BY
SATELLITE AND AIRBORNE MAGNETOMETERS OVER
WESTERN CANADA (NASA) 39 p HC A03/NF A01

N80-17527

Unclas
12897

CSCL 08G G3/43

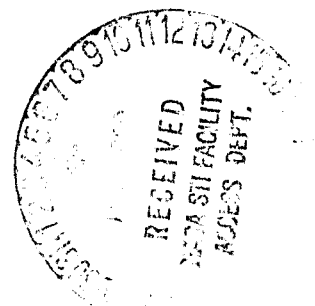
Comparison of Magnetic Anomalies of Lithospheric Origin Measured by Satellite and Airborne Magnetometers Over Western Canada

**R. A. Langel, R. Coles,
and M. A. Mayhew**

SEPTEMBER 1979

National Aeronautics and
Space Administration

Goddard Space Flight Center
Greenbelt, Maryland 20771



COMPARISONS OF MAGNETIC ANOMALIES OF LITHOSPHERIC
ORIGIN MEASURED BY SATELLITE AND AIRBORNE
MAGNETOMETERS OVER WESTERN CANADA

R.A. Langel¹

R.L. Coles²

M.A. Mayhew³

¹Geophysics Branch, NASA Goddard Space Flight Center, Greenbelt, MD 20771 USA

²Earth Physics Branch, Department of Energy, Mines and Resources,
Ottawa, Canada K1A 0Y3

³Business and Technological Systems, Inc., Seabrook, MD 20801 USA

ABSTRACT

Crustal magnetic anomaly data from the OGO 2, 4, and 6 (Pogo) satellites are compared with upward-continued aeromagnetic data between 50° - 85° N latitude and 220° - 260° E longitude. Agreement is good both in anomaly location and in amplitude, giving confidence that it is possible to proceed with the derivation and interpretation of satellite anomaly maps in all parts of the globe. The data contain a magnetic high over the Alpha ridge suggesting continental composition and a magnetic low over the southern Canada basin and northern Canadian Arctic islands (Sverdrup basin). The low in the Sverdrup basin corresponds to a region of high heat flow, suggesting a shallow Curie isotherm. A ridge of high field, with two distinct peaks in amplitude, is found over the northern portion of the platform deposits and a relative high is located in the central portion of the Churchill province. No features are present to indicate a magnetic boundary between Slave and Bear provinces, but a trend change is evident between Slave and Churchill provinces. South of 60° latitude a broad magnetic low is located over very thick (40-50 km) crust, interpreted to be a region of low magnetization.

INTRODUCTION

In recent years it has been realized that crustal magnetic anomalies exist which are of longer wavelengths than those investigated by exploration geophysicists and that these longer wavelength (greater than 50 km) anomalies are indicative of geologic and tectonic features in the deep crust (Pakiser and Zietz, 1965; Zietz et al., 1966; Shuey et al., 1973; Hall, 1974; Kruitkhovskaya and Paskevich, 1977).

With the publication of the paper by Regan et al. (1975) it was demonstrated that long wavelength lithospheric anomalies could be mapped successfully from satellites. That map showed a global distribution of anomalies of about 500-3000 km scale size which were never before mapped and whose very existence was in most cases discovered for the first time. Although this map was distorted by variations in altitude over the data set and by contamination from magnetospheric fields, Regan et al. were able to demonstrate that the probable source of the anomalies is indeed the lithosphere. Subsequently Regan and Marsh (1979) have collected ancillary data and derived a quantitative model of an anomaly located in central Africa. Analysis techniques for this type of data are rapidly becoming available (Bhattacharrya, 1977; Mayhew, 1978, 1979).

While analysis of data at lower latitudes has proceeded (Regan and Marsh, 1979; Mayhew, 1979), nothing has been published dealing with anomalies measured by satellite at the higher latitudes. The reason for this is that at low latitudes the external (magnetospheric/ionospheric) fields are mainly of longer wavelength than the anomalies being mapped, and can be readily

filtered from the data, thus isolating the anomaly fields. This remains true as long as data within about three hours of local noon are not utilized. At high latitudes, however, ionospheric currents occur at all local times and are very often present even during magnetically quiet periods of time. Further, these currents result in fields of the same spatial scale as the anomalies of interest, thus complicating the problem of isolating the anomaly fields. This paper is a report on an attempt to isolate the anomaly fields at satellite altitude for such high latitudes, and in particular over that part of Canada between 50°N - 85°N latitude and 220° - 260°E longitude. To gauge the success of this attempt, the resulting anomaly map is compared to aeromagnetic data upward continued to satellite altitude, 500 km.

THE SATELLITE DATA

A survey of the near-earth magnetic field was carried out by the Polar Orbiting Geophysical Observatories (OGO 2, 4 and 6), also known as the Pogo satellites (Langel, 1973; 1974). Some characteristics of the Pogo orbits are given in Table 1. OGO 2 acquired data from launch until October 2, 1967, OGO 4 from launch until January 19, 1969 and OGO 6 from launch until August 29, 1970 and then sporadically until June 1971. Each satellite completed about 15 revolutions each day. OGO 2 and OGO 4 acquired a data point every 0.5 seconds and OGO 6 every 0.288 seconds.

The measured magnetic field, \vec{B} , is the vector sum of magnetic fields from several sources. These are the main (core) field of the earth, \vec{M} , the variable field due to ionospheric and magnetospheric currents, \vec{D} , and the field originating in the lithosphere of the earth, \vec{A} . In this study the

main field is represented by a spherical harmonic model, \vec{M}_C , of degree and order thirteen designated Pogo(02/72) and described in the Appendix. It should be noted that this model is intended primarily as a representation of the main field of the earth for the time span of the Pogo data. The degree and order were chosen on the basis of studies by Phillips (unpublished, personal communication), Cain et al. (1974), and Cain (1976), which indicate that a 13th degree and order representation is sufficient to represent the main field without unduly distorting the anomaly field. Any such choice is, of course, a compromise and no exact separation is possible.

OGO 2, 4 and 6 measured the magnitude but not the direction of the field \vec{B} . The quantity analyzed is thus the residual field,

$$\Delta B = |\vec{B}| - |\vec{M}_C|.$$

This residual field contains contributions from: (1) any inaccuracy in modeling the core field \vec{M} with \vec{M}_C , (2) the external field, \vec{D} , and (3) the lithospheric field, \vec{A} . Contributions from \vec{D} are minimized by elimination of all data in which the residual field was considered to be dominantly due to \vec{D} . This elimination was accomplished on a pass by pass basis in two steps. (A pass is defined as a continuous set of data beginning when the satellite goes above 50° latitude and ending when it again goes below 50° on the other side of the pole.) First, if the magnitude of the residual field, ΔB , exceeds 20 nT (nanotesla) at any place in the pass, the entire pass is rejected. Second, the remaining passes are visually intercompared to attempt to distinguish the time invariant features, the lithospheric field $|\vec{A}|$, from the time

varying external field $|\vec{D}|$, and passes with significant contribution from the latter are not used in the anomaly map. A total of 271 "quiet" passes remained and were used in deriving the anomaly map. After performing these operations the internal agreement of passes which are nearly coincident geographically is substantial which indicates the presence and reality of the crustal anomalies. However, significant differences of wavelength more than 2-3 thousand kilometers still remain between coincident passes. This is similar to the results of Mayhew (1979) over the continental U.S. His solution was to remove a polynomial function separately from each individual pass. Only passes with several thousand km of data were used. This function is determined by a least squares fit to that pass. The procedure of Mayhew was followed with the data presented here except that Mayhew chose a quadratic function whereas we have chosen a linear function. The function chosen is a matter of subjective judgement. The difference between the linear and quadratic function for these data is not substantial. We are, of course, left with an anomaly field with arbitrary zero. After the data selection and trend removal, individual residual field data points were averaged in an equal-area grid superimposed over an equal area map of the area of interest. The grid is square and the distance along each side is equivalent to 3° of latitude. Figure 1 shows the density distribution of the data used in the averages. The resulting averaged residual anomaly map, contoured at 2 nT intervals, is shown in Figure 2a. Results in the southwest portion of the map, between 220° - 240° longitude and 50° - 60° N latitude are to be regarded with caution because of the sparseness of data as shown in

Figure 1. The residuals plotted in Figure 2a are not at a common altitude but are at the altitudes determined in each block over which the data were averaged. The average altitude varies from 440 to 560 km with mean near 520 km. A map reduced to common altitude is discussed later in the paper.

The anomalies range from a maximum of 14 nT at about 85° latitude to a minimum of -11 nT at 50° latitude and 239° longitude.

THE AIRBORNE MAGNETOMETER DATA

The airborne magnetic field data considered here have been acquired by the Earth Physics Branch of the Department of Energy, Mines and Resources, Ottawa, since 1969 in a series of airborne vector magnetometer surveys, each survey covering 2 to $4 \times 10^6 \text{ km}^2$ at a typical altitude of 3.5 km above sea level with excursions giving a range of 2.5-6.0 km. The instrumentation and survey details have been variously described by Haines and Hannaford (1972, 1974, 1976) and Hannaford and Haines (1974). Discussion of the data have been given by Haines et al. (1971), Riddihough et al. (1973), Coles et al. (1976), and Coles and Haines (1979).

The data were obtained in three separate surveys flown at approximately two year intervals. In order to remove level differences due to secular change, a reference field has been removed. Coles (1979) has shown that the best available reference field models for this region and for this interval of time are based on the Pogo data. The model chosen was the Pogo(02/72) model, i.e., the same reference field used for the satellite data. Coles also demonstrated a way of correcting for inadequacies in the secular change terms of the reference model in its application to the airborne data. The

residual data values are in effect adjusted to a single epoch. At each magnetic observatory in or near the survey region, the change in average quiet Jay field level from the epoch of the survey to the updated epoch is compared with the change in value of the field model between the two epochs. This comparison leads to a low-degree polynomial correction surface to be applied to the data residuals. The airborne data residuals were upward continued to 500 km in order to compare them with the satellite data. A fuller discussion of this procedure is given by Coles and Haines (1979). The input data to the upward continuation were in the form of averages of vertical component residuals along flight tracks over 5 minutes of time (about 35 km distance). The data points are shown in Figure 3, and Figure 4 is a contoured map prepared from the 5 minute averaged data.

The data averages were each associated with an area determined by the spacing (35 km) multiplied by the mean flight line spacing in the region of each data average. Although the original data were only along flight lines, the approximation is sufficient for the present purposes. No corrections for variations in flight altitude have been incorporated.

The basic equation for upward continuation from a sphere can be approximately represented, for the vertical component Z_p at point P, by

$$Z_p = \frac{R^2 - R_0^2}{4\pi R} \sum \frac{Z_i}{\rho_i^3} \Delta S_i$$

where the summation is over all data points i , each associated with an area ΔS_i and field value Z_i , R is the geocentric distance to the point P, R_0 is

the radius of the earth, and ρ_i is the distance from P to the point i. The data values, Z_i , are residuals relative to the reference field. The residual field beyond the data area is assumed to be zero and therefore has no contribution to the summation. This is an assumption, of course, which limits the accuracy of the upward continuation. Coles and Haines (1979) discuss this point in more detail: however, the actual total contribution from distant points beyond the data area is small (less than about 2 nT for most parts of the area), since the integral of the residual field over a large region tends to zero.

The data (5600 points) have been upward continued to 100 km, 300 km and 500 km (Figures 5 and 2b). As the altitude increases, the anomalies become smoother and reduced in amplitude. Broad features, however, persist through the series of figures.

COMPARISON OF THE ANOMALY MAPS

There is good agreement between the satellite and airborne data in their common spectral region. The agreement is excellent in the north, with a high anomaly north of 80°N , a low region between about 70° and 80°N , and a north-easterly trending ridge of high field centered near 65° - 67°N in the west and extending to about 70°N in the east. A south-trending relatively positive area extends between 55°N and 62°N at a longitude of about 240° . In the southwest the agreement is less good, with a large gradient evident in the airborne-derived map. Nevertheless, the indications are of a relatively low field over the southwestern Cordillera region in Canada. The agreement in

anomaly amplitudes is also very good, except in the southwest corner. This comparison gives a confirmation over a sub-continental size region of the reality of the anomalies derived from satellite data. This is particularly important for this region of the earth where contaminating fields from high latitude currents are strong and it indicates that we have been successful in separating the anomaly fields from fields due to those currents.

The reason for the discrepancy in the southwest between the two maps is not clear. The method of upward continuation is not a major factor since different analyses of the original data also indicate a similar discrepancy (Coles and Haines, 1979). The Pogo anomaly map is determined relative to a model also derived from Pogo data so one would not expect trends of ten to twenty nT to be present in that map. Either the available satellite data are consistently high in this region (the density of satellite passes is very low here), or the airborne data (one particular survey) are consistently low.

GEOLOGIC IMPLICATIONS

It is not our intention to present a detailed interpretation of the magnetic anomaly maps shown here. Interpretations of the aeromagnetic data have already been published (Haines et al., 1971; Riddihough et al., 1973; Coles et al., 1976). In this section we wish to contrast the different viewpoints offered by the aeromagnetic and satellite magnetic data and to illustrate the use of the satellite data in making geologic inferences.

Examination of Figure 4 shows changes in the character of the anomaly patterns from region to region, often delineating geologic boundaries. Such changes are clearly apparent between the Cordillera and the platform, i.e., between regions II and III and between the platform of region III and the thick sediments both onshore and offshore, of region IV. The character changes most evident are (1) changes from high magnetic relief to low magnetic relief and (2) changes in the trends of the anomalies. Because most of the high relief features are positive there is also an apparent contrast between regions of predominantly positive and predominantly negative fields. Figure 6 shows the satellite field, now reduced to common altitude using an equivalent source representation (Mayhew, 1978, 1979). In contrast to Figure 4, the satellite map shows only the contrasts between the predominantly positive and negative regions. The aeromagnetic data clearly contains all of the information in the satellite data and more and it is able to delineate boundaries more definitively. However, the satellite map (or an upward continued aeromagnetic map) gives a clearer picture of broad trends and can serve as a guide in discerning those same trends in the lower altitude data. In the following paragraphs we will discuss the various "regions" delineated by the satellite anomalies (Figure 6), compared with those delineated by the aeromagnetic data (Figure 4) and known geologic provinces.

At the very north of the map the satellite data shows a prominent high of about 12 nT magnitude. This is centered on the Alpha ridge of the Arctic Basin. The airborne survey also shows a broad positive in this region but is punctuated by a complex series of intense positive anomalies nearly

parallel to the trend of the ridge. These extend both north and south of the ridge and are all contained within the area of positive field as seen by Pogo. This region has also been surveyed by Vogt et al. (1979) who concluded that the principal magnetic anomalies in this region are topographic effects in a normally magnetized basement with high magnetization intensity (20-30 A/m). The broader picture afforded by the satellite data supports the existence of a region of highly magnetized crust and partially outlines its extent. Unfortunately, the satellite data do not extend above 87° latitude so the northern portion of this region is not mapped. The upward continued aeromagnetic data indicate that it terminates at about 88° latitude.

The Alpha ridge has been variously interpreted as a subduction zone (Herron et al., 1974), as an extinct center of sea-floor spreading (Churkin, 1973; Vogt and Ostenso, 1970; Hall, 1973; Tailleux, 1973; Vogt and Avery, 1974), or as subsided continental crust (Eardley, 1961; King et al., 1966; Taylor, 1978). DeLaurier (1978) rejects the hypotheses of a subduction zone or a center of sea-floor spreading on the basis of a comparison of the measured relief with the relief expected from a cooling model, because of a lack of seismic activity, and because active accretion is inconsistent with the known marine fossils and sediment thickness. Vogt et al. (1979) also examine these questions and conclude that on the basis of the airborne magnetic data it is not possible to rule out any of the three hypotheses. In addition to the arguments noted above against a spreading center or subduction zone they claim that the depth of the Alpha ridge argues against it being a subsided shield.

Taylor (1978) suggests that the Alpha ridge is an aseismic ridge similar to the Lord Howe Rise, which is continental in nature, in the southwest Pacific. In fact, the satellite data show a similar positive anomaly over the Lord Howe Rise (Regan et al., 1975). Coles et al. (1978) and Sweeney et al. (1978) note that the positive long-wavelength anomaly over the Alpha ridge is consistent with a region of crust of continental composition since most of the major long-wavelength positive anomalies detected by satellites are associated with continental crust, both in shield areas and in regions such as Broken Ridge in the Indian Ocean (Regan et al., 1975).

To the south of the Alpha ridge and its environs the satellite map shows a broad negative over the southern Canada Basin and the northern Canadian Arctic Islands. The aeromagnetic data in this region are remarkably free from shorter wavelength anomalies. Geologically this is a region of deep (3-12 km) sediments (Sweeney et al., 1978) resulting in a greater depth to basement which may account for the lack of shorter wavelength anomalies in the aeromagnetic data (Riddihough et al., 1973). The southern zero nT contour of this region is close to the edge of the craton but both bathymetric (Sweeney et al., 1978) and seismic (Sweeney et al., 1978; Berry and Barr, 1971; Sander and Overton, 1965; Overton, 1970; Berry, 1973) data show that the transition from continental to oceanic crust, the Canada Basin, takes place well within the region of negative anomaly. Comparison of Figure 6 with the bathymetry (Sweeney et al., 1978) indicates that over much of its length the -4 nT contour nearly coincides with the continental slope. Thus the central low of the negative anomaly is located over oceanic crust.

The eastward extension of this magnetic low is over the Sverdrup Basin where refraction data (Sander and Overton, 1965; Overton, 1970; Forsyth et al., 1979) indicate sediments reaching 12 km. Forsyth et al. note that "Based on heat flow measurements taken in bore-holes throughout the Sverdrup Basin, A.S. Judge has estimated that maximum temperatures are 600 to 650°C at 20 km and 850 to 900°C at 30 km (personal communication)." Judge noted higher than average heat flow values for the central Sverdrup Basin. Thus the magnetite Curie isotherm is well up into a thickly sedimented crust in this region which could account for the relative negative magnetic anomaly. The cause of the negative anomaly over the Canada Basin is unknown. Future refinement of the satellite data over the rest of the Arctic will be required to see if the negative anomaly is co-extensive with the entire Amerasian Basin.

An elongated region of high magnetic field (Figure 6) is located near 65° latitude at 220°E longitude in the west and extends to 71° latitude at 260°E longitude. This "high" occurs over the northern portion of the platform deposits on the Precambrian craton and can be resolved into two maxima. In the east the positive anomaly extends southward over the northern parts of the exposed shield. Considering the two highs over the platform deposits, comparison with Figure 4 shows positive anomalies in the aeromagnetic data in these regions but of significantly different character. In the east, over Victoria Island, there is no concentration of short-wavelength anomalies whereas in the west the broad positive background is punctuated by narrow regions of intense positive short-wavelength anomalies. This region of large

amplitude anomalies extends around the top of region II (Figure 4) and has been interpreted to indicate that the crystalline continental basement extends far to the west of the exposed and known buried shield (Coles et al., 1976). This regional difference seems to be reflected in the heat flow data (although a good thermal model is not yet available and the available data are sparse) in that the available heat flow values near the western field maximum are considerably higher than those near the eastern maximum. This difference in heat flow between two magnetic highs of nearly equal amplitude indicates that the long wavelength anomalies, at least to the east of the Cordillera, do not correlate well with heat flow and therefore are not indicative of variations in the depth to the Curie isotherm. For comparison, in the United States good heat flow vs long wavelength anomaly correlation is evident in the tectonically active region west of the Cordillera (Mayhew, in preparation) whereas in the more stable region to the east of the Cordillera the extremely sparse heat flow data do not seem to correlate with the long wavelength magnetic anomalies.

Just to the south of the double maximum the contour lines are relatively featureless with a northeasterly trend. In particular no features are present marking the boundary between Bear and Slave provinces. Below 67° latitude a trend change is evident between Slave and Churchill provinces and, near the eastern border of the map, a relative high extends through the central portion of the Churchill province. This relative high is not clearly defined in the aeromagnetic data, which do not extend as far east as the satellite data.

South of about $60-63^{\circ}$ the satellite anomaly map is everywhere negative, highly negative in some regions. The low altitude data of Figure 4 show that large portions of this area are relatively free of large amplitude short-wavelength anomalies. A relative negative anomalous region can be caused by one or a combination of three things: very low rock magnetization, a shallow Curie isotherm, or a high reversed remanent magnetization. The latter is extremely unlikely for a geographic region of this size; reversed magnetizations for regions this size are neither expected nor found in practice. Although sparse, the existing heat flow data are at or below normal values with no indication of a shallow Curie isotherm. Thus the crust in this region, which is 40-50 km thick (Chandra and Cumming, 1972; Berry, 1973), most likely has very low average rock magnetization over most of its area. The satellite data shows a relative high at about $57-60^{\circ}$ latitude and $238-241^{\circ}$ longitude. This is reflected in the low altitude aeromagnetic data (Figure 4) as a cluster of magnetic highs east of the Cordillera, and in fact the Cordillera is outlined by their western boundary. Most of this region of "highs" is underlain by sedimentary cratonic cover rocks, reaching several kilometers thickness in the west. Some deep drill holes exist to the east of the Cordillera within both the area of short-wavelength intense positive anomalies and the area further southeast, free of such anomalies. The magnetizations of basement rocks from the bottoms of the drill holes have been measured (R.A. Burwash, personal communication, 1974; R.L. Coles, unpublished data, 1975). Although sparse, the magnetization values outside

the area of short-wavelength positive anomalies are lower on average than what appears to be typical for shield areas, whereas within the area of short-wavelength "highs," much of the crystalline basement is highly magnetic.

SUMMARY

Aeromagnetic and satellite magnetic data have been presented and compared for western Canada. Such a comparison at these geomagnetic latitudes is important because both data types are affected by fields from external (ionospheric and magnetospheric) sources. Such external fields are particularly troublesome to the satellite data where, even after careful data selection, external fields are undoubtedly present on most data passes. The close agreement between the two data types indicates that it is possible to extract the anomaly "signal" from the satellite data and that the anomalies so defined are indeed crustal in origin. We believe it is now possible to proceed in confidence with the derivation and interpretation of satellite anomaly maps in all parts of the globe.

Both averaging of satellite data and upward continuation of aeromagnetic data serve to filter out details in the field. For aeromagnetic data this is not a problem since one can compare with results for lower altitudes. Derivation of an equivalent source representation of the satellite data preserves most of the information content of the data, as is apparent from comparison of Figure 6 and Figure 2a. Broad interpretive comparison of the equivalent source field with known geologic and geophysical data has indicated

that it is indeed indicative of important features in the crust and can aid in solution of such problems as the nature and origin of the Alpha ridge and the nature of the crystalline basement underlying sedimentary cover.

APPENDIX

The spherical harmonic analysis used to represent the earth's main field in this study is designated Pogo(2/72). The data set utilized in the derivation of this field model is identical to that used for the Pogo(8/71) field model (Langel, 1973; 1974) except that no data from 1970 were used in the derivation of Pogo(2/72). The fitting procedure used 47,485 data points that were fit with the coefficients given in Table 2 to a root mean square residual of 6.2 gamma. The distribution of residuals is given in Table 3, and pertinent statistics relative to data from the three satellites in Table 4.

The model generation assumed a spheroidal earth with mean radius of 6371.0 km, equatorial radius of 6378.16 km, and a flattening factor of $1/298.25$.

Because it was not designed as a predictive model, Pogo(2/72) does not include data from observatories to aid in determination of the secular variation. It is, however, suitable for some uses at times past 1971. Mead (1979) has recently evaluated four field models for the epoch 1973-1976, well past the time span of the data utilized to create the models. The models evaluated were Pogo(8/71), IGS/75 (Barracough et al., 1975), AWC/75 (Peddie and Fabiano, 1976) and IGRF 1975 (IAGA, 1976). He concluded that

the first three were all about equally accurate and much superior to IGRF 1975. Both AWC/75 and IGS/75 are slightly better than Pogo(8/71). An extension of Mead's result shows that Pogo(2/72) is of comparable accuracy to Pogo(8/71) for the epoch 1973-1976.

ACKNOWLEDGEMENTS

We would like to thank M.K. Hutchinson, R. Horner and D. Love for their efforts in data preparation and display and G.D. Mead and P.T. Taylor for valuable discussion and review of the manuscript.

FIGURE CAPTIONS

Figure 1: Density of distribution of Pogo data.

Figure 2: Comparison of (a) Averaged magnetic anomalies from Pogo data with (b) upward continued aeromagnetic anomaly data.

Figure 3: Relative distribution of aeromagnetic data.

Figure 4: Residuals of aeromagnetic data at an altitude of 3 km. Roman numerals designate regions of differing characteristics as described in the text.

Figure 5: Upward continuation of aeromagnetic data.

Figure 6: Reduction of Pogo anomaly map to an altitude of 500 km using an equivalent source representation. The contour interval is 1 nT.

TABLE 1. SOME CHARACTERISTICS OF THE POGO ORBITS

| <u>SATELLITE</u> | <u>LAUNCH DATE</u> | <u>INCLINATION</u> | <u>PERIGEE, km</u> | <u>APOGEE, km</u> |
|------------------|--------------------|--------------------|--------------------|-------------------|
| OGO 2 (1965 81A) | October 14, 1965 | 87.3 ⁰ | 410 | 1510 |
| OGO 4 (1967 73A) | July 28, 1967 | 86.0 ⁰ | 410 | 910 |
| OGO 6 (1969 51A) | June 5, 1969 | 82.0 ⁰ | 400 | 1100 |

TABLE 2. POGO (2/72) COEFFICIENTS, EPOCH 1960
units are nT and nT/yr.

| <u>n</u> | <u>m</u> | <u>g_n^m</u> | <u>h_n^m</u> | <u>\dot{g}_n^m</u> | <u>\dot{h}_n^m</u> |
|----------|----------|---------------------------|---------------------------|---------------------------------|---------------------------------|
| 1 | 0 | -30456.2 | 0.0 | 23.47 | 0.0 |
| 1 | 1 | -2180.3 | 5819.0 | 12.67 | -8.84 |
| 2 | 0 | -1546.2 | 0.0 | -23.09 | 0.0 |
| 2 | 1 | 2996.2 | -1994.0 | 0.53 | -4.20 |
| 2 | 2 | 1605.2 | 203.2 | -2.19 | -17.71 |
| 3 | 0 | 1304.8 | 0.0 | -2.29 | 0.0 |
| 3 | 1 | -1982.6 | -443.9 | -11.86 | 8.18 |
| 3 | 2 | 1305.6 | 222.6 | -2.08 | 3.02 |
| 3 | 3 | 886.7 | -156.7 | -5.50 | -2.99 |
| 4 | 0 | 961.4 | 0.0 | -1.11 | 0.0 |
| 4 | 1 | 811.7 | 136.7 | -1.15 | 2.96 |
| 4 | 2 | 496.7 | -276.6 | -2.69 | 0.96 |
| 4 | 3 | -381.7 | 16.2 | -1.05 | 0.54 |
| 4 | 4 | 264.5 | -259.9 | -2.66 | -1.39 |
| 5 | 0 | -222.7 | 0.0 | 0.89 | 0.0 |
| 5 | 1 | 358.9 | 11.7 | 0.30 | 0.98 |
| 5 | 2 | 242.9 | 118.4 | 1.52 | 1.75 |
| 5 | 3 | -28.1 | -111.4 | -0.97 | -2.99 |
| 5 | 4 | -140.6 | -101.2 | -2.37 | 0.84 |
| 5 | 5 | -95.2 | 119.1 | 4.86 | -3.81 |
| 6 | 0 | 46.0 | 0.0 | -0.02 | 0.0 |
| 6 | 1 | 59.1 | -9.0 | 0.32 | -0.21 |
| 6 | 2 | -0.1 | -106.8 | 1.36 | -0.46 |
| 6 | 3 | -243.2 | 61.5 | 2.83 | 1.28 |
| 6 | 4 | -3.3 | -26.5 | 0.58 | -1.42 |
| 6 | 5 | -0.1 | -20.3 | 0.11 | 1.59 |
| 6 | 6 | -102.1 | -4.4 | -1.01 | 0.30 |
| 7 | 0 | 71.1 | 0.0 | -0.15 | 0.0 |
| 7 | 1 | -51.6 | -52.9 | -0.29 | -1.68 |
| 7 | 2 | 3.9 | -27.3 | -0.32 | 0.18 |

| | | | | | |
|----|----|-------|-------|-------|-------|
| 7 | 3 | 12.3 | -7.2 | 0.28 | 0.11 |
| 7 | 4 | -39.9 | 1.4 | 1.85 | 1.01 |
| 7 | 5 | 0.9 | 17.6 | -0.46 | 0.36 |
| 7 | 6 | -4.0 | -35.1 | 2.25 | 1.80 |
| 7 | 7 | 39.7 | -47.5 | -5.78 | 4.11 |
| 8 | 0 | 8.9 | 0.0 | 0.36 | 0.0 |
| 8 | 1 | 3.9 | 11.1 | 0.24 | -0.35 |
| 8 | 2 | -4.6 | -12.7 | 0.41 | -0.20 |
| 8 | 3 | -11.0 | 8.8 | -0.01 | -0.48 |
| 8 | 4 | -0.3 | -15.4 | -0.51 | -0.34 |
| 8 | 5 | 6.2 | 8.1 | 0.04 | -0.36 |
| 8 | 6 | -5.5 | 19.6 | 0.34 | 0.14 |
| 8 | 7 | 12.3 | 6.1 | 0.01 | -1.44 |
| 8 | 8 | -6.8 | -35.1 | 1.49 | 2.05 |
| 9 | 0 | 11.4 | 0.0 | -0.31 | 0.0 |
| 9 | 1 | 7.8 | -22.0 | 0.12 | -0.0 |
| 9 | 2 | 3.4 | 14.7 | -0.26 | -0.01 |
| 9 | 3 | -12.3 | 2.1 | 0.01 | 0.42 |
| 9 | 4 | 17.0 | 1.2 | -0.73 | -0.51 |
| 9 | 5 | 1.2 | -1.7 | -0.22 | -0.25 |
| 9 | 6 | 8.1 | 18.5 | -1.15 | -1.30 |
| 9 | 7 | -9.1 | 18.2 | 1.70 | -0.90 |
| 9 | 8 | 10.3 | 4.7 | -1.09 | -1.09 |
| 9 | 9 | -6.5 | 8.6 | 1.45 | -1.06 |
| 10 | 0 | -2.1 | 0.0 | 0.05 | 0.0 |
| 10 | 1 | -1.7 | 3.5 | -0.14 | -0.17 |
| 10 | 2 | 1.5 | 0.3 | 0.05 | 0.07 |
| 10 | 3 | -4.1 | 0.3 | -0.05 | 0.17 |
| 10 | 4 | -3.4 | 4.8 | 0.22 | 0.14 |
| 10 | 5 | 9.3 | -2.7 | -0.42 | -0.14 |
| 10 | 6 | 5.7 | 2.2 | -0.12 | -0.20 |
| 10 | 7 | 2.8 | -5.4 | -0.33 | 0.38 |
| 10 | 8 | 0.6 | 8.7 | -0.04 | -0.67 |
| 10 | 9 | 0.9 | -7.0 | 0.39 | 0.91 |
| 10 | 10 | 4.0 | -9.3 | -0.48 | 0.63 |

| | | | | | |
|----|----|------|-------|-------|-------|
| 11 | 0 | 2.4 | 0.0 | 0.01 | 0.0 |
| 11 | 1 | -0.2 | 1.3 | -0.09 | 0.01 |
| 11 | 2 | -1.9 | 2.6 | 0.00 | 0.04 |
| 11 | 3 | 5.0 | -1.8 | -0.17 | -0.00 |
| 11 | 4 | -2.4 | -4.2 | 0.20 | -0.19 |
| 11 | 5 | -1.2 | 1.5 | 0.18 | 0.14 |
| 11 | 6 | -4.0 | -3.9 | 0.47 | 0.54 |
| 11 | 7 | 3.7 | -1.0 | -0.28 | -0.05 |
| 11 | 8 | -0.0 | -3.0 | 0.33 | 0.44 |
| 11 | 9 | -0.7 | -5.3 | -0.26 | 0.37 |
| 11 | 10 | -3.6 | -3.8 | 0.80 | 0.36 |
| 11 | 11 | 5.4 | -8.7 | -0.28 | 1.28 |
| 12 | 0 | -0.5 | 0.0 | -0.15 | 0.0 |
| 12 | 1 | 0.3 | 1.1 | -0.03 | -0.08 |
| 12 | 2 | 0.4 | 0.1 | -0.13 | 0.05 |
| 12 | 3 | 0.2 | 1.9 | -0.02 | 0.03 |
| 12 | 4 | 1.6 | 0.3 | -0.15 | -0.10 |
| 12 | 5 | 0.4 | -0.6 | 0.02 | 0.04 |
| 12 | 6 | 0.1 | 0.4 | -0.11 | -0.02 |
| 12 | 7 | -2.3 | -1.3 | 0.20 | 0.13 |
| 12 | 8 | 0.7 | -1.3 | -0.04 | 0.25 |
| 12 | 9 | 0.3 | 2.7 | -0.13 | -0.30 |
| 12 | 10 | -0.5 | -0.6 | 0.06 | -0.07 |
| 12 | 11 | -4.4 | 4.8 | 0.44 | -0.55 |
| 12 | 12 | -5.4 | -4.6 | 0.80 | 0.40 |
| 13 | 0 | 1.1 | 0.0 | -0.10 | 0.0 |
| 13 | 1 | 0.7 | 1.8 | -0.15 | -0.23 |
| 13 | 2 | 0.7 | 0.7 | -0.00 | -0.05 |
| 13 | 3 | -0.6 | 0.6 | 0.00 | 0.06 |
| 13 | 4 | 1.0 | -0.3 | -0.09 | 0.00 |
| 13 | 5 | 0.7 | -0.7 | -0.03 | 0.08 |
| 13 | 6 | 0.9 | 0.9 | -0.13 | -0.19 |
| 13 | 7 | -1.0 | -0.2 | 0.10 | 0.09 |
| 13 | 8 | 0.8 | 0.1 | -0.16 | -0.10 |
| 13 | 9 | 2.2 | 0.3 | -0.20 | 0.06 |
| 13 | 10 | 3.5 | 3.6 | -0.49 | -0.45 |
| 13 | 11 | -1.5 | 6.9 | 0.17 | -0.79 |
| 13 | 12 | -8.5 | -6.2 | 0.88 | 0.63 |
| 13 | 13 | 3.3 | -11.4 | -0.15 | 1.14 |

TABLE 3: DISTRIBUTION OF RESIDUALS

| Range (gamma) | -50 to -50 | -50 to -40 | -40 to -30 | -30 to -20 | -20 to -10 | -10 to 0 | 0 to 10 | 10 to 20 | 20 to 30 | 30 to 40 |
|------------------|------------|------------|------------|------------|------------|----------|---------|----------|----------|----------|
| Number of Points | 2 | 4 | 25 | 216 | 2562 | 19113 | 23692 | 1831 | 28 | 2 |

TABLE 4: STATISTICS FOR OGO-2, OGO-4, AND OGO-6

| | NUMBER OF PTS. | RMS (gamma) | MEAN (gamma) | STANDARD DEVIATION ABOUT MEAN (gamma) |
|-------|----------------|-------------|--------------|---------------------------------------|
| OGO-2 | 12773 | 5.17 | 0.263 | 5.16 |
| OGO-4 | 18431 | 6.80 | 0.088 | 6.80 |
| OGO-6 | 16281 | 6.25 | -0.063 | 6.21 |

REFERENCES

- Barracclough, D.R., Harwood, J.M., Leaton, B.R., and Malin, S.R.C. 1975. A model of the geomagnetic field at epoch 1975. *Geophysical Journal of the Royal Astronomical Society*, 43, pp. 645-659.
- Berry, M.J. 1973. Structure of the crust and upper mantle in Canada. *Tectonophysics*, 20, pp. 183-201.
- Berry, M.J. and Barr, K.G. 1971. A seismic refraction profile across the polar continental shield of the Queen Elizabeth islands. *Canadian Journal of Earth Sciences*, 8, pp. 360-374.
- Bhattacharyya, B.K. 1977. Reduction and treatment of magnetic anomalies of crustal origin in satellite data. *Journal of Geophysical Research*, 82, pp. 3379-3390.
- Cain, J.C. 1976. Introductory remarks. Abstract. *EOS, Transactions of the American Geophysical Union*, 57, p. 907.
- Cain, J.C., Davis, W.M., and Regan, R.D. 1974. An N=22 model of the geomagnetic field. Abstract. *EOS, Transactions of the American Geophysical Union*, 56, p. 1108.
- Chandra, N.N. and Cumming, G.L. 1972. Seismic refraction studies in western Canada. *Canadian Journal of Earth Sciences*, 9, pp. 1099-1109.
- Churkin, M. 1973. Geologic concepts of Arctic Ocean Basin, in *Arctic Geology*. (M.G. Pitiha, Ed.). American Association of Petroleum Geology, Memoir 1a, pp. 485-499.
- Coles, R.L. 1979. Some comparisons among geomagnetic field models, observatory data and airborne magnetometer data: implications for broad scale anomaly studies over Canada. *Journal of Geomagnetism and Geoelectricity* (in press).

- Coles, R.L., Haines, G.V., and Hannaford, W. 1976. Large scale magnetic anomalies over western Canada and the Arctic: a discussion. *Canadian Journal of Earth Sciences*, 13, pp. 790-802.
- Coles, R.L., Hannaford, W., and Haines, G.V. 1978. Magnetic anomalies and the evolution of the Arctic. In Arctic Geophysical Review, (J.F. Sweeney, Ed.). Publication of the Earth Physics Branch, Energy, Mines and Resources, Ottawa, Canada, 45, pp. 51-66.
- Coles, R.L. and Haines, G.V. 1979. Long-wavelength magnetic anomalies over Canada, using polynomial and upward continuation techniques. *Journal of Geomagnetism and Geoelectricity* (in press).
- DeLaurier, J.M. 1978. The Alpha Ridge is not a spreading centre. In Arctic Geophysical Review, (J.F. Sweeney, Ed.). Publication of the Earth Physics Branch, Energy, Mines and Resources, Ottawa, Canada, 45, pp. 87-90.
- Eardley, A.J. 1971. History of geologic thought on the origin of the Arctic Basin. In Geology of the Arctic (G.O. Raesh, Ed.). University of Toronto Press, Toronto, pp. 223-249.
- Forsyth, D.A., Mair, J.A., and Fraser, I. 1979. Crustal structure of the central Sverdrup basin. *Canadian Journal of Earth Sciences* (in press).
- Haines, G.V. and Hannaford, W. 1972. Magnetic anomaly maps at British Columbia and the adjacent Pacific Ocean. Publication of the Earth Physics Branch, Energy, Mines and Resources, Ottawa, Canada, 42(7), pp. 211-228.
- Haines, G.V. and Hannaford, W. 1974. A three-component aeromagnetic survey of the Canadian Arctic. Publication of the Earth Physics Branch, Energy, Mines and Resources, Ottawa, Canada, 44(8), pp. 209-234.

- Haines, G.V. and Hannaford, W. 1976. A three-component aeromagnetic survey of Saskatchewan, Alberta, Yukon and the District of Mackenzie. Earth Physics Branch Geomagnetic Series No. 8, Ottawa, Canada, 34 p.
- Haines, G.V., Hannaford, W., and Riddihough, R.P. 1971. Magnetic anomalies over British Columbia and the adjacent Pacific Ocean. Canadian Journal of Earth Sciences, 8, pp. 387-391.
- Hall, D.H. 1974. Long-wavelength aeromagnetic anomalies and deep crustal magnetization in Manitoba and north western Ontario, Canada. Journal of Geophysics, 40, pp. 403-430.
- Hall, J.K. 1973. Geophysical evidence for ancient sea floor spreading from Alpha Cordillera and Mendeleyev Ridge. In American Association of Petroleum Geology (M.G. Pitcher, Ed.). American Association of Petroleum Geology, Memoir 19, Tulsa, Oklahoma.
- Hannaford, W. and Haines, G.V. 1974. A three-component aeromagnetic survey of British Columbia and the adjacent Pacific Ocean. Publication of the Earth Physics Branch, Energy, Mines and Resources, Ottawa, Canada, 44(14), pp. 323-379.
- Herron, E.M., Dewey, J.F., and Pitman, W.C., III. 1974. Plate tectonics model for the evolution of the Arctic. Geology, pp. 377-380.
- IAGA Division 1 Study Group. 1976. International Geomagnetic Reference Field 1975. EOS, Transactions of the American Geophysical Union, 57, pp. 120-121.
- King, E.R., Zietz, I. and Alldredge, L.R. 1966. Magnetic data on the structure of the central Arctic region. Geological Society of America Bulletin, 77, pp. 619-646.

- Kruitkhovskaya, A.A., and Paskevich, I.K. 1977. Magnetic model for the earth's crust under the Ukrainian shield. *Canadian Journal of Earth Sciences*, 14, pp. 2718-1728.
- Langel, R.A. 1973. A study of high latitude magnetic disturbance. Technical Note BN-767, Institute for Fluid Dynamics and Applied Mathematics, University of Maryland, College Park, Maryland.
- Langel, R.A. 1974. Near-earth magnetic disturbance in total field at high latitudes 1. Summary of data from OGO 2, 4, and 6. *Journal of Geophysical Research*, 79, pp. 2363-2371.
- Mayhew, M.A. 1978. A computer program for reduction of Pogo satellite magnetic anomaly data to common elevation and to the pole. Contract Report, NASA Contract NAS 5-41625-B.
- Mayhew, M.A. 1979. Inversion of satellite magnetic anomaly data. *Journal of Geophysics*, 45, pp. 119-128.
- Mead, G.D. 1979. An evaluation of recent internal field models. In Quantitative Modeling of Magnetospheric Processes (W.P. Olson, Ed.). *Geophysics Monograph*, 21, pp. 110-117.
- Overton, A. 1970. Seismic refraction surveys, western Queen Elizabeth islands and polar continental margin. *Canadian Journal of Earth Sciences*, 7, pp. 346-363.
- Pakiser, L.C. and Zietz, I. 1965. Transcontinental crustal and upper mantle structure. *Review of Geophysics*, 3, pp. 505-520.
- Peddie, N.W. and Fabiano, E.B. 1976. A model of the geomagnetic field for 1975. *Journal of Geophysical Research*, 81, pp. 2539-2542.

- Regan, R.D., Cain, J.C. and Davis, W.M. 1975. A global magnetic anomaly map. *Journal of Geophysical Research*, 80, pp. 794-802.
- Regan, R.D. and Marsh, B.D. 1979. The Bangui anomaly: its geological origin. Submitted to *Journal of Geophysical Research*.
- Riddihough, R.P., Haines, G.V., and Hannaford, W. 1973. Regional magnetic anomalies of the Canadian Arctic. *Canadian Journal of Earth Sciences*, 10, pp. 147-163.
- Sander, G.W. and Overton, A. 1965. Deep seismic refraction investigations in the Canadian Arctic archipelago. *Geophysics*, 30, pp. 87-96.
- Shuey, R.T., Schellinger, D.R., Johnson, E.H., and Alley, L.G. 1973. Aeromagnetics and the transition between the Colorado Plateau and the Basin Range province. *Geology*, 1, pp. 107-110.
- Sweeney, J.F., Coles, R.L., DeLaurier, J.M., Forsyth, D.A., Irving, E., Judge, A., Sobczak, L.W., and Wetmiller, R.J. 1978. Arctic geophysical review - A summary. Publication of the Earth Physics Branch, Energy, Mines and Resources, Ottawa, Canada, 45, pp. 101-108.
- Tailleux, I.L. 1973. Probable rift origin of Canada Basin, Arctic Ocean. In *Arctic Geology* (M.G. Pitcher, Ed.). Memoir 19. American Association of Petroleum Geology, pp. 526-535.
- Taylor, P.T. 1978. Low-level aeromagnetic data across the western arctic basin. Abstract. EOS, Transactions of the American Geophysical Union, 59, p. 268.

- Vogt, P.R. and Ostenso, N.A. 1970. Magnetic and gravity profiles across the Alpha Cordillera and their relations to arctic sea floor spreading. *Journal of Geophysical Research*, 75, pp. 4925-4937.
- Vogt, P.R. and Avery, O.E. 1974. Tectonic history of the Arctic Basins: Partial solutions and unsolved mysteries. In *Marine Geology and Oceanography of the Arctic Seas* (Y. Hermann, Ed.). Springer-Verlag, New York. pp. 83-117.
- Vogt, P.R., Taylor, P.T., Kovacs, L.C., and Johnson, G.L. 1979. Detailed aeromagnetic investigation of the arctic basin. *Journal of Geophysical Research*, 84, pp. 1071-1089.
- Zietz, I., King, E.R., Geddes, W., and Lidiak, E.G. 1966. Crustal study of a continental strip from the Atlantic Ocean to the Rocky Mountains. *Geological Society of America Bulletin*, 77, pp. 1427-1448.

NUMBER OF POINTS IN AVERAGES

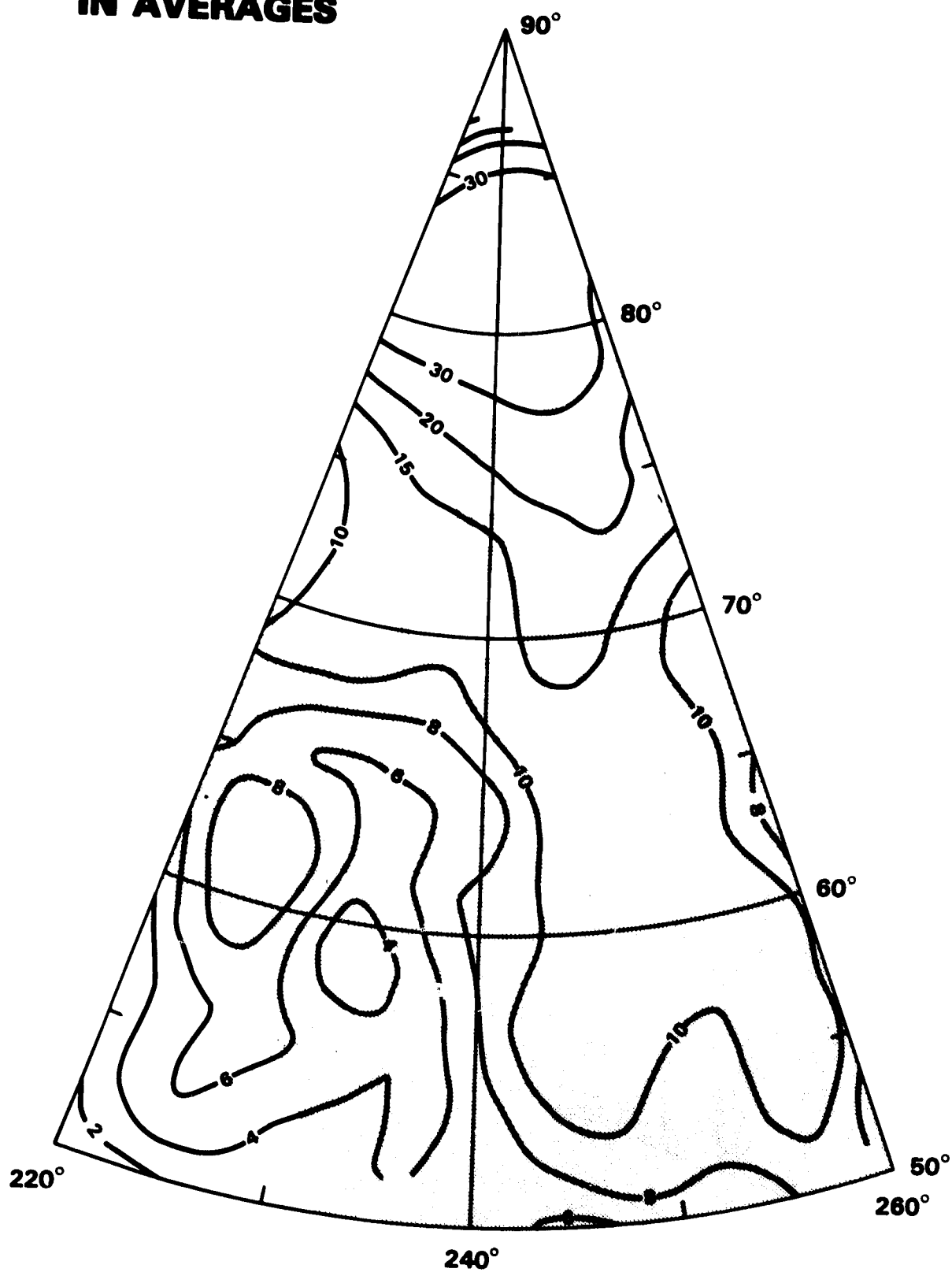


Figure 1

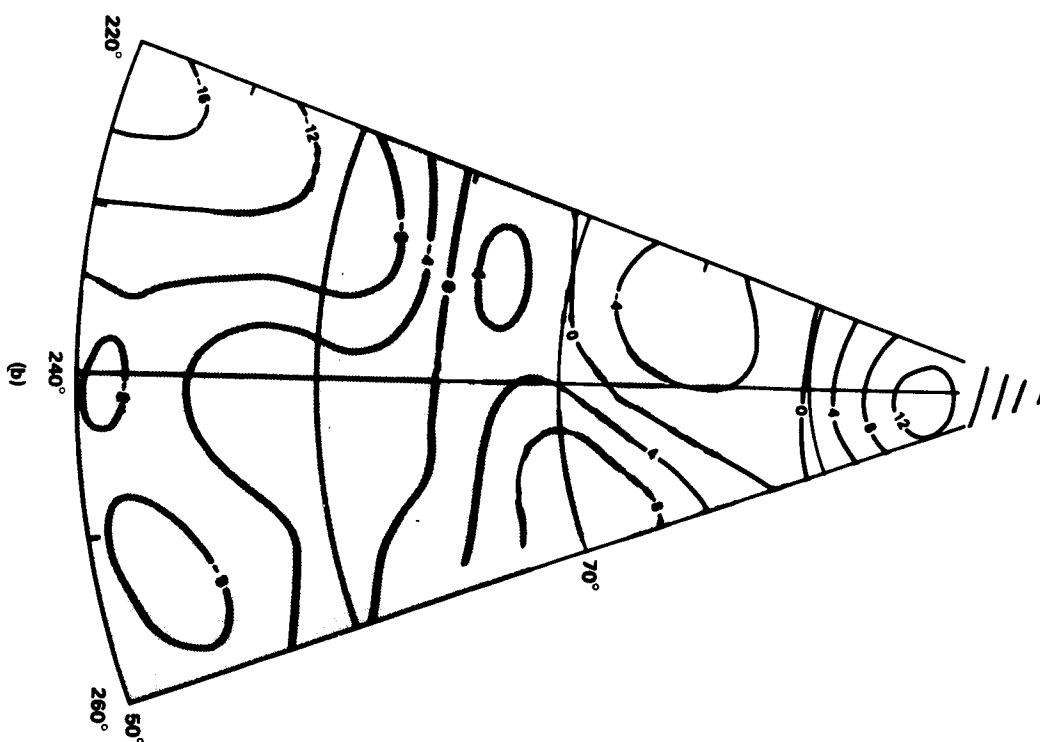
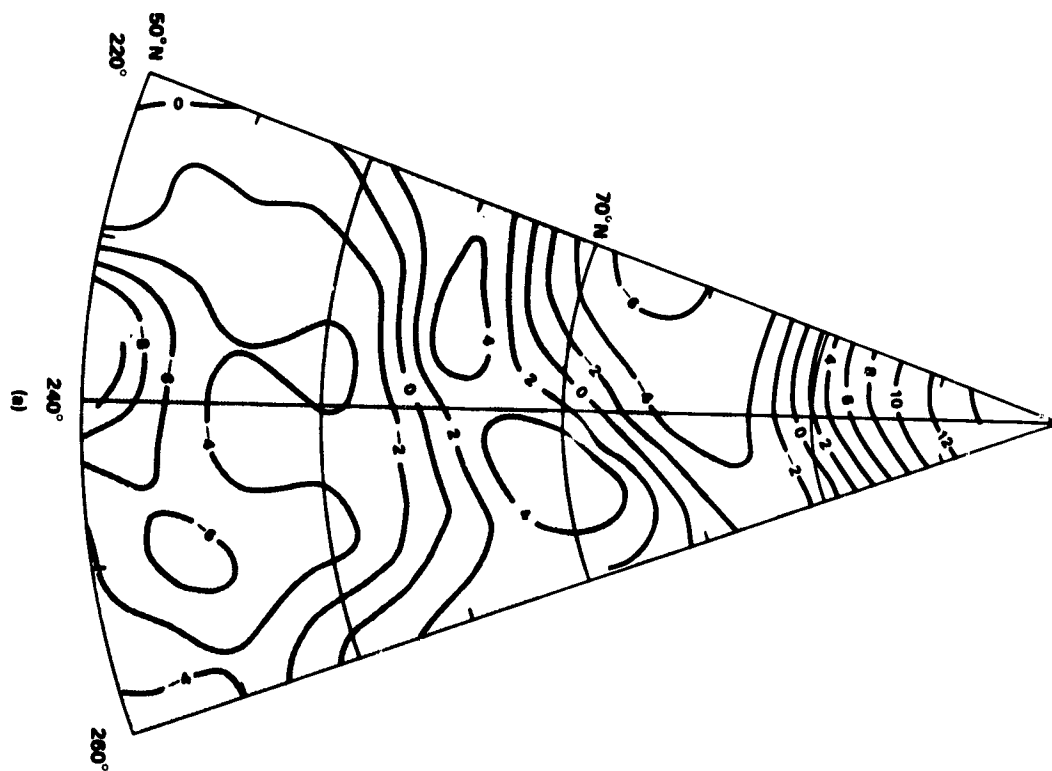


Figure 2

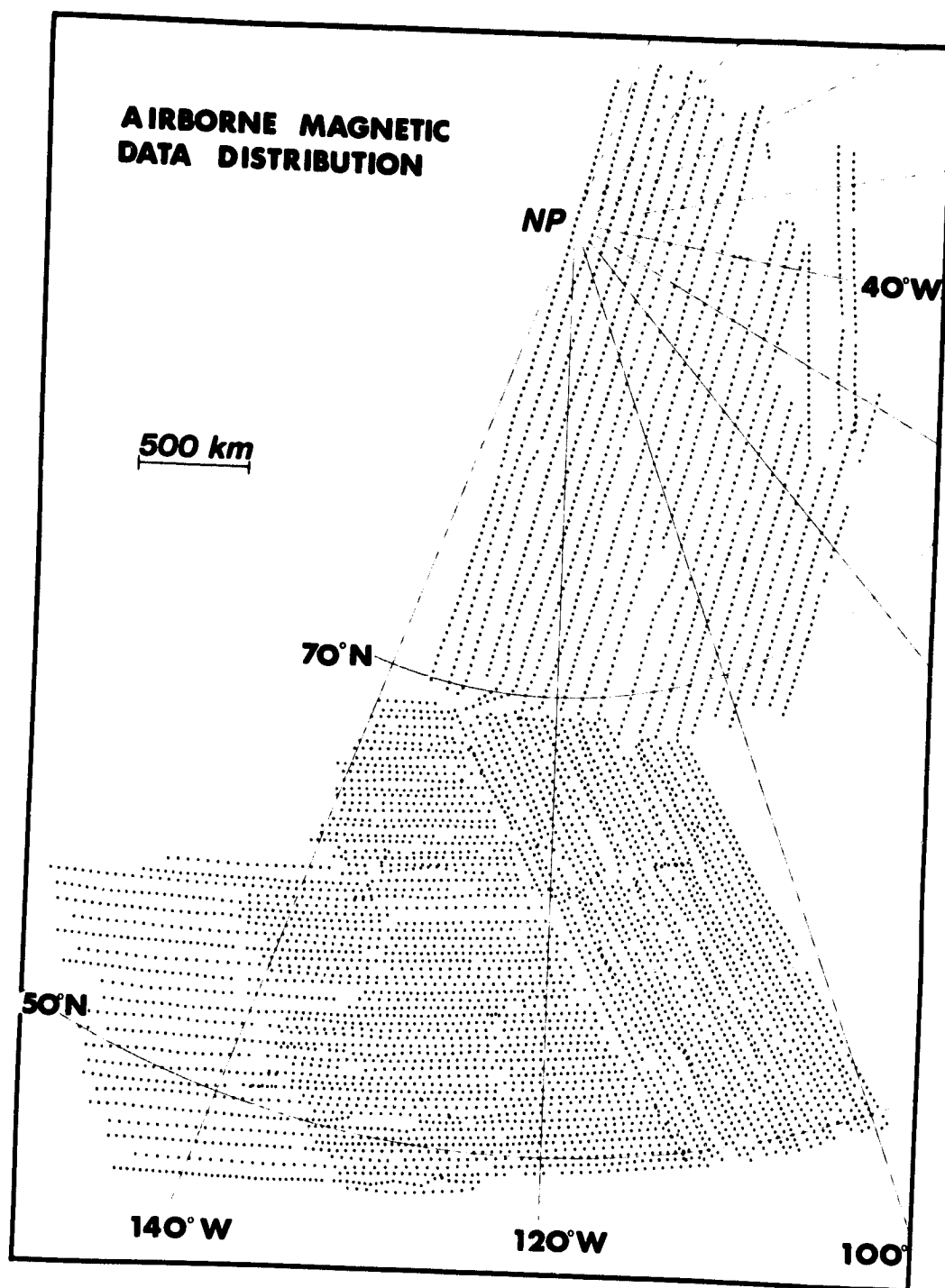


Figure 3

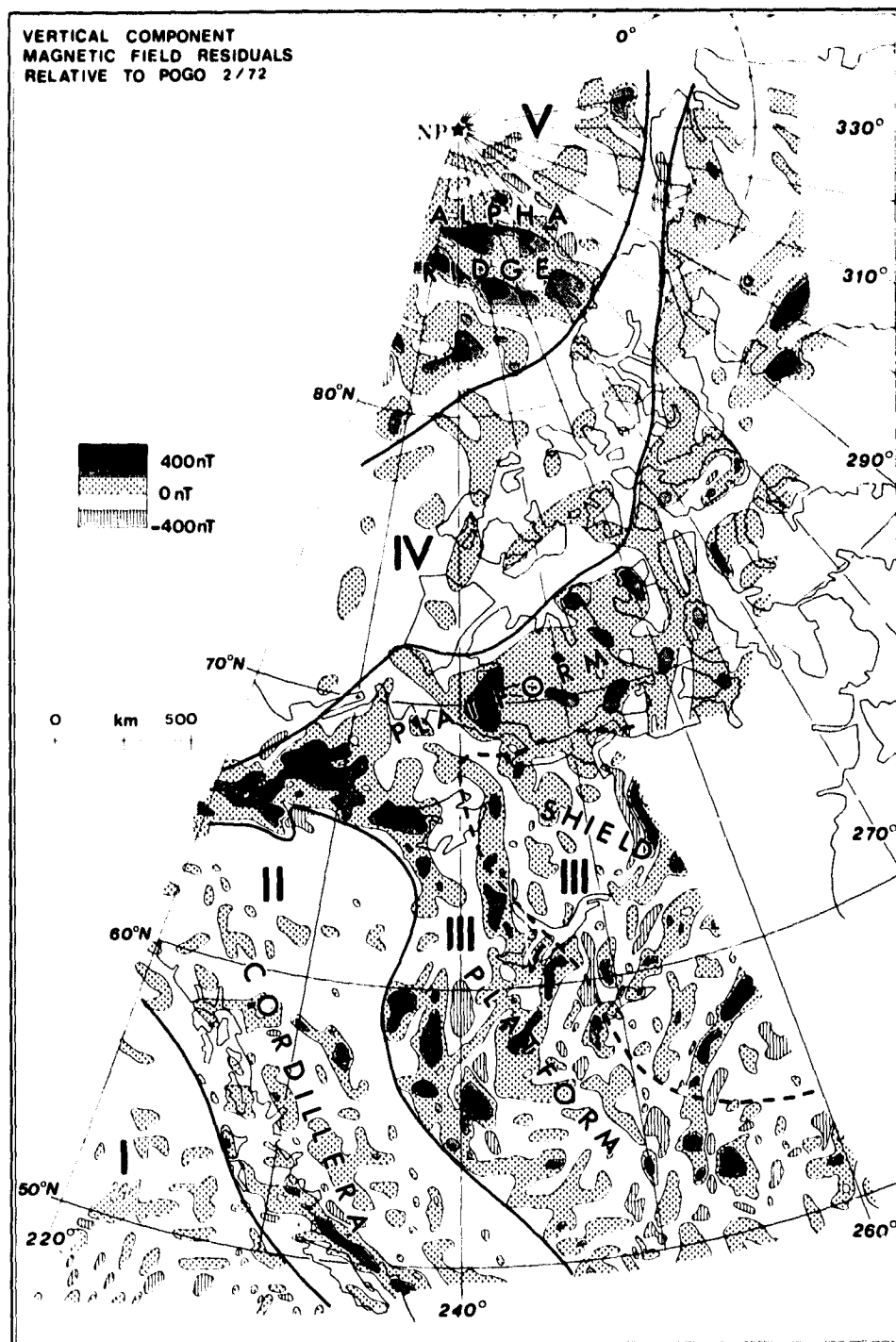


Figure 4

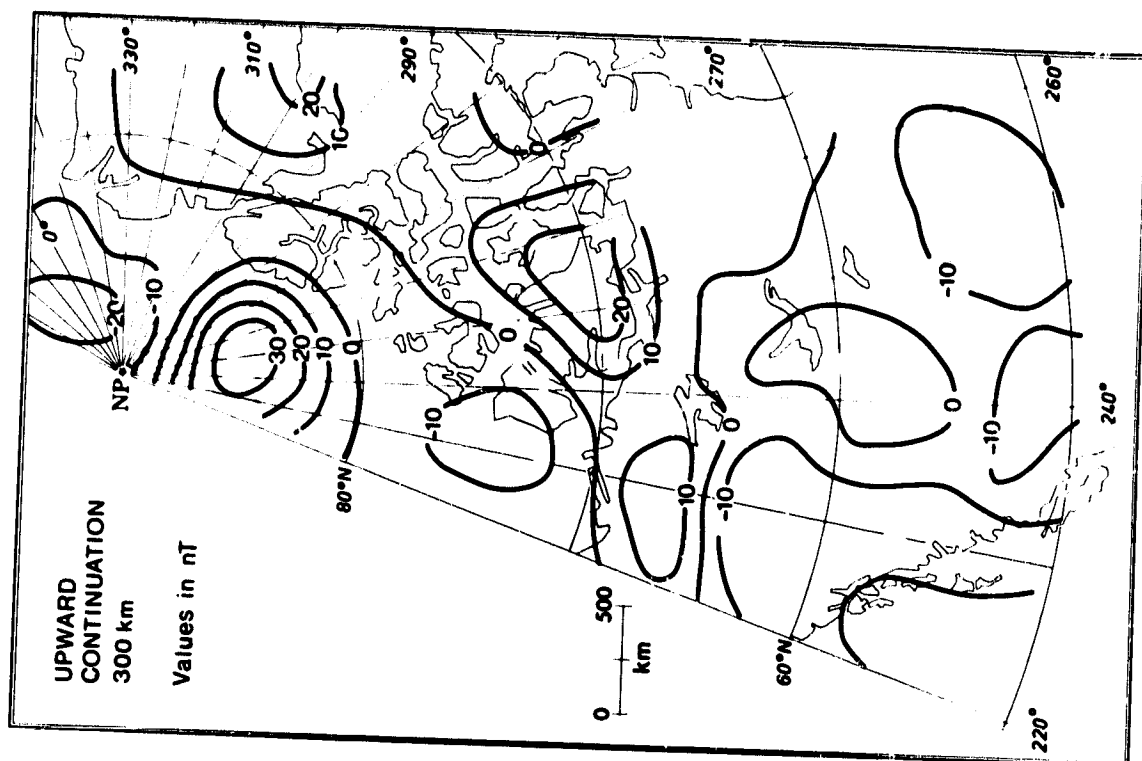
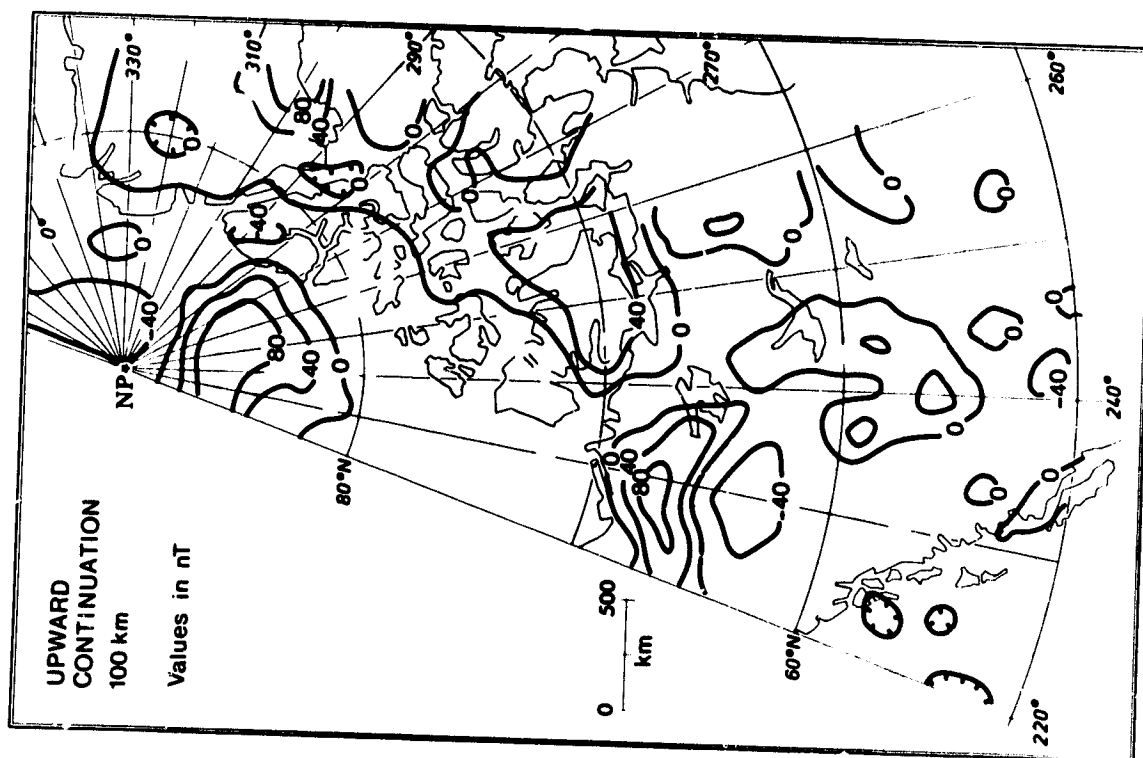


Figure 5

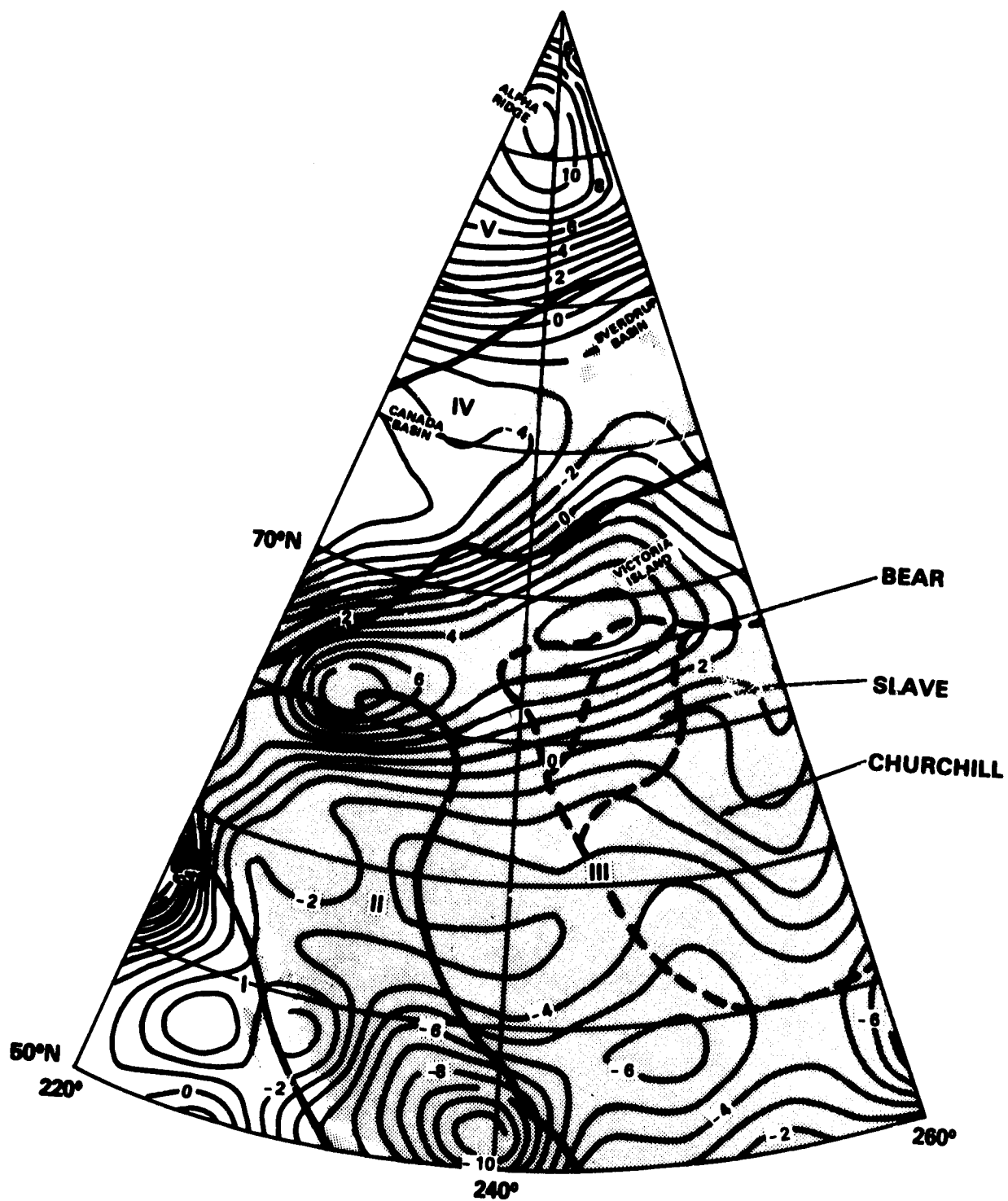


Figure 6